Producing carbon nanotubes from thermochemical conversion of waste plastics using Ni/ceramic based catalyst

Xiaotong Liu[a], Boxiong Shen[b*], Zhentao Wu[c*], Christopher M. A. Parlett[d*], Zhenan Han[e], Adwek George[b], Peng Yuan[b], Dipesh Patel[a], Chunfei Wu[a,b,f*]

[a] School of Engineering and Computer Science, Faculty of Science and Engineering, University of Hull, Hull, HU6 7RX

[b] School of Energy and Environmental Engineering, Hebei University of Technology, Tianjin, China

[c] Aston Institute of Materials Research, School of Engineering and Applied Science, Aston University, Birmingham B4 7ET, UK

[d] European Bioenergy Research Institute, Aston University, Birmingham, B4 7ET, UK

[e] Wuhan Optics Valley Environmental Technology Co., Ltd, Wuhan City, China 430074

[f] School of Chemistry and Chemical Engineering, Queen's University Belfast, Belfast, BT7 1NN, UK

Corresponding authors: Tel: +44 (0) 1482466464, Email: c.wu@hull.ac.uk; Tel: +86 (0) 2260435784, E-mail: shenbx@hebut.edu.cn; Tel: +44 (0) 121204 3353, Email: z.wu7@aston.ac.uk; Tel: +44 (0)1212 044100 c.parlett@aston.ac.uk)

Abstract

As the amount of waste plastic increases, thermo-chemical conversion of plastics provides an economic flexible and environmental friendly method to manage recycled plastics, and generate valuable materials, such as carbon nanotubes (CNTs). The choice of catalysts and reaction parameters are critical to improving the quantity and quality of CNTs production. In this study, a ceramic membrane catalyst (Ni/Al_2O_3) was studied to control the CNTs growth, with reaction parameters, including catalytic temperature and Ni content investigated. A fixed two-stage reactor was used for thermal pyrolysis of plastic waste, with the resulting CNTs characterized by various techniques including scanning electronic microscopy (SEM), transmitted electronic microscopy (TEM), temperature programmed oxidation (TPO), and X-ray diffraction (XRD). It is observed that different loadings of Ni resulted in the formation of metal particles with various sizes, which in turn governs CNTs production with varying degrees of quantity and quality, with an optimal catalytic temperature at 700 °C.

Keywords: Plastics waste; Carbon nanotubes; ceramic membrane; Nickel; catalyst

1. Introduction

There was more than 4.3 million tonnes plastics waste generated in the UK in 2015 [1], the disposal of waste plastic causes environmental concerns. Therefore, careful management is needed to minimize the environmental impact of plastic waste. As waste plastic contains a high value of energy, recycle and recovery methods are encouraged compared to landfilling. Thermochemical recycling of waste plastics which converts plastics materials into other valuable materials, refers to an advanced technology process [2]. During this process, hydrogen-rich syngas is generated at high pyrolysis temperature (>800 °C) or gasification of waste plastics. For example, Erkiaga et al. [3] generated a syngas stream rich in H_2 from pyrolysis of plastic waste (high density polyethylene) with Ni catalysts. Syngas has wide applications, including directly combusted for the production of heat and power, or conversion into liquid fuels through Fishcher-Tropsch process [4]. Recently, co-production of carbon nanotubes (CNTs) from pyrolysis or gasification of waste plastics has also attracted interest. CNTs were first introduced in 1952, and further inspired by Iijima [5, 6]. CNTs have extraordinary properties, including high mechanical strength, good electrical and thermal conductivity, and there promising potential applications. However, the high price (~$85-95/kg) has significantly prohibited the applications of CNTs [7]. Converting plastic waste to CNTs provides a promising alternative and economic flexible method to generate such high valuable material.

Chemical vapour deposition (CVD) is the current method of choice and widely utilised

53 to produce CNTs from plastics, due to its simplicity and low cost. This method used
54 hydrocarbon gases as carbon sources and catalysts particles to nucleate the CNTs
55 growth [8]. For example, Park et al. [9] optimized operation conditions with Ru-based
56 catalysts from waste plastic, in order to decrease the coke formation and increase the
57 carbon conversion. Liu et al. [10] used a two-stage reactor to convert PP into CNTs and
58 hydrogen-rich gas with HZSM-5 as catalysts, and an optimum temperature (700°C)
59 was proposed. Wu et al. studied the production of CNTs and syngas study from different
60 types of plastics with varies of catalysts [11-14].

61 It is known that catalysts play a key role in the growth of CNTs. The catalysts used for
62 CVD synthesis of CNTs formation normally consist of a transition metal and support.
63 The transition metal nanoparticles are employed either in oxide or metallic forms.
64 Nickel, iron, and cobalt are reported as the most effective catalysts due to the high
65 solubility and high diffusion rate of carbon. For example, Lee et al [15] compared the
66 performance of Ni, Co and Fe based catalysts for CNTs growth from mixed gases. Fe
67 was found to be the most active catalyst for CNTs growth under CO/NH_3 gas flow with
68 a ratio of 18. Apart from these common catalysts, there are also some other types of
69 metals that have been studied for CNTs formation, such as Cu, Ru, Mn and Cr. Catalysts
70 for CNTs formation also need an appropriate material as support [16]. Various
71 substrates have been used for CVD of CNTs synthesis, such as silicon dioxide [14],
72 alumina [17], quartz, calcium carbonate [18], and zeolite [19]. Fe-Co bimetallic
73 catalysts supported on $CaCO_3$ were used as catalysts by Mhlanga et al. [18] to improve
74 the quality of CNTs with decreasing synthesis time from acetylene. CNTs with outer

diameter of 20-30 nm and inner diameter about 10 nm have been successfully produced. Furthermore, many researchers are working on catalyst development to improve the quality of CNTs [13, 20-24].

Recently, membrane supported catalysts have emerged, and can be used as a template for CNTs growth to control parameters such as diameter, length, and wall thickness [25]. For example, Golshadi et al. [25] investigated the influence of process parameters (temperature and flow rate) on the CNTs formation (tube wall thickness, CNTs morphology and carbon deposition rate) using anodic aluminum oxidize (AAO) template. It was reported that the yield and wall thickness of the produced CNTs were increased with the increase of reaction temperature to 750 °C; however, further increasing the temperature resulted in a lower production of CNTs. In addition an optimum of gas flow rate was reported for the production of CNTs. Well-aligned CNTs have also been synthesized on glass template from acetylene gas by plasma-enhanced CVD process [26]. Zeolites have also been employed as controlling agents during CNTs growth [27].

According to our previous study, AAO membrane catalysts could be used for controlling and improving the quality of CNTs formation [28]. Ceramic membrane (alumina based) was selected as template in this study. This ceramic membrane was provided by AIMR, Aston University, and the properties were studied in Lee's paper [29]. In Lee's paper, ceramic membrane was reported having micro-channel structure, which was similar to our previous research on AAO membrane [28] [29]. This micro-

channel structure could control the metal particle loaded inside the membrane and consequently control the CNTs diameter. However, the yield of CNTs production using AAO based membrane is low as AAO is difficult to be manufactured in a large scale. Ceramic membrane has been commercially produced and also has other good properties, such as high temperature stability, mechanical strength, chemical stability, and low cost [30, 31]. These properties make ceramic materials one of the best catalytic supports in the fields of environmental and energy research [31]. Quan et al. produced high quality syngas from biomass fuel gas over NiO/porous ceramic catalysts [32]. And Gao et al. studied steam reforming of biomass tar for hydrogen production using NiO/ceramic foam as catalysts [33]. Membrane catalysts have also shown superior catalytic stability over equivalent powder [34].

The quality of CNTs can significantly affect and limit their applications. For example, An et al. [35] synthesized CNT composite from the catalytic decomposition of acetylene over Fe/aluminum ceramic catalyst. It was reported that the CNT content increased with the increase of Fe content. The mechanical properties of the produced composite material was also enhanced with the increase of CNTs formation. Flahaut et al. [36] prepared Fe-Al_2O_3 ceramics with and without CNTs to study composites properties, and they found those contained higher quantities of CNTs and much less nanofibers were good electric conductors. Therefore, experimental conditions (both reaction temperature and Ni loading) were studied to determine the optimal conditions for the production of high quality CNTs, which is reflected by a narrow distribution of CNTs diameter.

2. Experimental

2.1 Materials preparation

Waste high density polyethylene plastics (HDPE) pellets was used as feedstock with high purity (~ 90%) and a diameter around 2 mm provided by Poli Plastic Pellets Ltd. Ceramic membrane used in this study was made of aluminium oxide, and with 1mm thickness and 30mm diameter provided by AIMR, Aston University. The original ceramic membrane preparation and formation method was described in Lee's paper [29]. It is noted that the BET surface area of the membrane is below 10 m^2/g. Impurities such as polyethersulfone was used as binder for membrane preparation. The required amounts (0.025g for 0.1/ceramic, 0.125g for 0.5/ceramic, 0.251g for 1.0/ceramic, 0.508g for 2.0 ceramic) of Ni $(NO_3)_2.6H_2O$ were dissolved in 5ml ethanol, the mixture liquid was loaded on each membrane (~1.32g) by dropping the precursors into the membrane. The obtained wet Ni/ceramic membrane was dried in the oven at 100℃ for 24h, then calcined in air at 800 ℃ with 10 ℃ min^{-1} heating rate for 3 hours. It is noted that the Ni/ceramic catalysts prepared from using 0.1, 0.5, 1.0 and 2.0 mol L^{-1} Ni $(NO_3)_2.6H_2O$ was assigned as 0.1/ceramic, 0.5/ceramic, 1.0/ceramic and 2.0/ceramic, respectively in this paper.

2.2 CNTs synthesis from catalytic pyrolysis of plastics

A two-stage catalytic thermal-chemical conversion reaction system (Fig. 1) consisting of a plastic pyrolysis stage and a catalytic gasification stage. In each experiment, about

1 g HDPE was pyrolysed at around 500 °C at the first stage, Different reaction temperatures were used in the second stage (600 °C, 700 °C, and 800 °C). N_2 was used as carrier gas with 100 ml min^{-1} flow rate. The total reaction time was 60 mins. The system was then slowly cooled down to the room temperature with continuous 100 ml min^{-1} N_2 gas. The reacted Ni/ceramic membrane catalyst including the grown CNTs were collected for further characterizations. The effect of pyrolysis temperature and the content of Ni on ceramic membrane were studied in relative to their influences on the growth of CNTs.

2.3 Sample characterization

A scanning electron microscope (SEM) Stereoscan 360 and a high resolution transmission electron microscope (TEM) JEOL 2010 were used to analyse the surface and the cross-section morphology of the fresh Ni/ceramic membrane. According to TEM results, the distribution of diameters of catalyst particles were further analyzed by Image J software. Sample crystallinity was evaluated by powder X-ray diffraction (XRD), using Stoe IPDS2 software, with elemental analysis assessed by inductively coupled plasma mass spectrometry (ICP-MS), ThermoScientific iCAP 7000 ICP spectrometer after complete sample digestion in conc. Nitric acid. In addition, temperature programmed reduction (TPR) was carried out on a Quantachrome Chem BET 3000 system, with samples heated from 50 °C to 700 °C at 10 °C min^{-1} under flowing H_2 (10 ml min^{-1}), to observe the catalytic metal reduction.

CNTs formation on the Ni/ceramic after reaction was also investigated by SEM and

TEM. Distribution of CNTs diameters according to TEM results was carried out using Image-J software. Temperature programmed oxidation (TPO) of the reacted Ni/ceramic was analysed to obtain the information of carbon formation on the reacted catalyst.

3. Results and discussion

3.1 Characterization of fresh Ni/ceramic catalyst

Fresh catalysts before reaction with different Ni loadings have been analysed by SEM, TEM, ICP, XRD and TPR, respectively. SEM results of the surface and the cross section of the fresh Ni/ceramic catalyst are shown in Fig. 2A and 2B, respectively. The surface and cross-section show a similar structure; porous structure can be clearly observed from both pictures. Therefore, SEM images on the surface of materials are used for following discussion. Based on the XRD results (Fig. 3), the original ceramic membrane without Ni loading shows diffraction peaks of Al_2O_3 [37], indicating the nature of the ceramic is Al_2O_3. NiO peaks appear at 63° and 76°, respectively, for the catalyst with different Ni contents loadings [14]. Two $NiAl_2O_4$ peaks appear at around 37° and 77° [38]. ICP results as shown in Table 1 further indicate that the content of Ni element increased from 0.25 to 3.3 wt. % with the increase of Ni loading. Fig. 4 shows the TEM results (A-D) for the Ni/ceramic samples. The distribution of NiO diameters was also calculated according to TEM results for the catalyst with different Ni loadings. Small amount of NiO particles was observed on the surface of the 0.1/ceramic, which has particles with 11.4 ± 2.4 nm diameter, with NiO diameter correlating with metal

loading, in agreement with the literature[11], resulting in average particle size of 35.2 ± 3.5 nm for the 2.0/ceramic (Fig.3 D).

TPR results of the fresh Ni/ceramic catalysts are shown in Fig. 5. A major reduction temperature for all the catalysts occurred between 370 and 450ºC, assigned to the reduction of NiO particles [11]. As shown in Fig. 5, the catalysts were further reduced at 550 ºC [11], which is suggested to the reduction of Ni spinel as observed from the XRD analysis (Fig.3).

3.2 Carbon nanotubes production

Two reaction parameters using ceramic membrane catalysts with different Ni contents loading were investigated in relation to the effect on the CNTs formation from plastics waste. Table 2 is a summary of different reaction parameters (Ni content and reaction temperature) and CNTs formation analysis (amount of amorphous carbon, filamentous carbon and CNT average diameter). When the effect of reaction temperature (600, 700, and 800 °C) was studied, the 0.5/ceramic catalyst was used. When the effect of Ni content (0.1, 0.5, 1.0 and 2.0) was studied, thermochemical conversion of waste HDPE was investigated at 700 °C.

CNTs formation from thermochemical conversion of plastics waste in this study was investigated according to both quantitative analysis and qualitative analysis. The quantitative analysis of CNTs was further discussed based on the yields of amorphous carbons and filamentous carbons which was obtained by TGA-TPO analysis of the spent catalysts (Fig. S1 and S2). It is assumed that the oxidation temperature below

550 °C was assigned to amorphous carbons and the oxidation above 550 °C in TPO was assigned to filamentous carbon (assumed as CNTs in this work) [39], two different types of carbon has been separated and analysed by vertical black imaginary line (Fig. S1 and S2). The total carbon yield could be represented by X axis 'the weight loss' of catalyst in relation to the initial catalyst weight. The fractions of the two different types of carbons in relation to the weight of reacted catalysts are summarized in Table 2.

In addition, the quality of CNTs production is analysed and discussed mainly based on the distribution of CNTs diameters and their standard deviations. The average diameter of CNTs is calculated according to SEM and TEM results using Image J, and summarized in Table 2 (shown in Fig. S3). The standard deviation (SD) number is used as a main factor to identify the quality of CNTs formation in this study. In addition, the ratio of filamentous and amorphous carbon was also discussed in following sections to obtain the optimum reaction parameter for CNTs formation. A better quality of CNTs is identified with a smaller SD number and higher ratio of filamentous and amorphous carbon in this paper.

3.3 Effect of reaction temperature on CNTs growth

The effect of reaction temperature on the growth of CNTs through thermal conversion from HDPE using Ni/ceramic catalysts is discussed in this section. Three different reaction temperatures (600°C, 700°C and 800°C) were investigated using the 0.5/ ceramic catalyst. Scanning electron microscope (SEM), transmitted electron microscope (TEM), temperature programmed oxidation (TGA-TPO and DTG-TPO)

223 analysis were carried out to the reacted CNTs/catalysts. For SEM results (Fig.6 A-C), a
224 small amount of uninform, short filamentous carbons were observed at 600°C (Fig.6A).
225 CNTs, which has a diameter ~10 nm and a length ~10 μm, is observed at catalytic
226 reaction temperature of 600 °C. This result is consistent with a previous study, which
227 used Ni/Al_2O_3 as catalysts to produce CNTs from waste plastics [14].

228 With the increase of reaction temperature to 700°C (Fig.6B), a large amount of
229 filamentous carbons with long length are found on the ceramic membrane. However,
230 when the reaction temperature was further increased to 800°C, only a few filamentous
231 carbons could be observed on the surface of the catalyst (Fig.6C). The SEM results of
232 the reacted catalyst were further supported by TEM analysis (Fig. 6 i-iii). CNTs with
233 diameter 21.2 ± 5.6 and 16.9 ± 4.3 nm were clearly observed in Fig. 6 i and ii,
234 respectively. It is difficult to find CNTs on the catalyst reacted at 800 °C (Fig.6 iii).
235 Therefore, it is suggested that 700 °C is an optimal reaction temperature for the
236 formation of CNTs from waste plastics in this work. Similar results were reported by
237 Li et al [40], who studied various temperatures from 600°C to 1050°C for CNTs
238 production from C_2H_2 with Fe/SiO_2 catalysts. They reported minimal CNTs yield at
239 either low (600°C) or high (1050°C) temperature.

240 This result is further supported by carbon production analysis (Table 2). For amorphous
241 carbons (oxidation temperature below 550 °C), the yield was decreased from 2.1 to 1.2
242 wt. %, when the temperature increased from 600 °C to 700 °C. This result is consistent
243 with the SEM analysis (Fig. 6), where amorphous carbons could be clearly observed on

244 the reacted catalyst tested at 600 °C. Furthermore, the formation of CNTs was reduced
245 from 7.2 wt. % and 1.2 wt. % when the reaction temperature was increased 600°C and
246 800°C. DTG-TPO results (Fig.7) with DCS (Differential Scanning Calorimetry)
247 showed that the oxidation peak moved to higher temperature with the increase of
248 experimental temperature from 600°C and 700°C, indicating that the CNTs might be
249 more crystalized at 700°C reaction temperature. Similar results were also reported by
250 Hornyak et al. [41], who investigated the template synthesis of CNTs formation on
251 porous alumina membrane (PAM) from propylene gas with Co-based catalysts. They
252 reported that amorphous carbon was formed at around 550°C, while CNTs was formed
253 at temperature higher than 800ºC. The starting temperature for CVD synthesis of CNTs
254 was normally over 500°C [42-44].

255 It is suggested that the effect of reaction temperature on CNTs synthesis by CVD was
256 mainly related to carbon source and catalytic sites. CNTs growth can be described as
257 following steps, first carbon atoms from the dissociation of hydrocarbons dissolve into
258 the catalytic metal sites. The diffused carbon atoms form graphitic sheets on the surface
259 of metal particles [45]. The diffusion of carbon atoms is a main factor to determine the
260 CNTs formation. The increasing temperature can promote the diffusion rate of carbon
261 atoms, as a result, CNTs are synthesised with less defect. Lee et al. [46] and Mishra et
262 al. [47] also reported that an increase of temperature promoted the diffusion and
263 reaction rates of carbons, resulting in the enhanced formation of CNTs. In addition, Wu
264 and Williams [48] reported that at high temperature, more reactive carbon sources were
265 produced from pyrolysis of waste plastics. Therefore, in this study, less amorphous

carbons were form at 700°C compared to 600°C, which supported by SEM and TPO analysis. Similar results were reported by Acomb et al. [49] who carried out the effect of growth temperature (700 °C, 800 °C, and 900 °C) on the CNTs production using low density polyethylene (LDPE) with Fe/Al_2O_3 as catalyst. They found that a lower temperature produced less fraction of CNTs.

However, when the reaction temperature is too high, the sintering of catalytic sites could occur, which is responsible for the deactivation of catalysts [43]. Also, the excess of carbon atoms accumulated on the surface of catalyst could encapsulate catalytic sites causing catalyst deactivation. For example, Hanaei et al. [50] investigated the influence of reaction temperatures (550°C-950°C) on CNTs from acetone with $Fe\text{-}Mo/Al_2O_3$ catalysts. 750°C was reported as an ideal temperature as the deactivation of catalysts occurred at higher temperature. Toussi et al. [51] reported the similar conclusion on CNTs synthesis form ethanol deposited on Fe-Mo-MgO catalyst; when temperature was lower than 750°C, few CNTs could be produced. And the optimum growth of CNTs was reported at 850°C. Kukoitsky et al. [52] reported an optimal temperature of 700°C for the growth of CNTs from polyethylene with Ni-based catalyst at 700°C; as narrow size distribution of CNTs was found at 700°C than those grown at 800°C, due to the loss of catalytic activity for CNTs forming at high temperature. In this study, it is noticed that there was little CNTs formed at 800ºC (Fig. 6 and 7), which we attribute to loss of catalytic active sites at high temperature due to sintering As shown in Fig. 6iii, almost no CNTs production could be observed from TEM results. The diameter of NiO particles before reaction was 17.9±4.4 nm (Fig. 4B), however, large amount of large

288 catalytic particles with diameter 52-78 nm could be observed after reaction (Fig. 6iii).
289 Overall, Fig. 8 summarizes the trends of SD of CNTs diameter and ratio of filamentous
290 amorphous carbon as increasing reaction temperature. CNTs show the smallest SD and
291 highest filamentous / amorphous carbon ratio at 700 °C reaction temperature. Therefore,
292 700°C was assumed as the optimum temperature for this study.

293 3.4 Effect of Ni content on the production of CNTs

294 In this section, thermochemical conversion of waste HDPE was investigated in the
295 presence of Ni/ceramic catalysts with different Ni contents at 700ºC. Fig.8 showed the
296 SEM results and corresponding TEM results for the filamentous carbon production
297 using the Ni/ceramic catalysts. With the increase of Ni loading, more filamentous
298 carbons could be observed from SEM results. In particular, for the reacted 0.1/ceramic
299 catalyst, the formation of filamentous carbons can be barely found. It is indicated that
300 the 0.1/ceramic and 0.5/ceramic catalysts might have small amount of active metals
301 loaded on the ceramic membrane. TEM results (Fig.8 i-v) further proved that the
302 filaments carbons are mostly CNTs. The average diameter of CNTs (Table 2) was
303 analysed according to the TEM results. It could be noticed that the diameter of CNTs
304 increased with an increase of Ni content. The 0.1/ceramic had the smallest diameter
305 15.7±3.6 nm, and the 2.0/ceramic had the largest diameter 24.9±2.3 nm, in close
306 agreement with the average sizes of the NiO nanoparticles. The changes of diameters
307 of CNTs showed a similar trend with the metal particles size as shown in Fig. 10, where
308 the particle size of NiO was increased with the increase of metal loading. Similar results

were also found by other researchers [53]. Sinnott et al. [53] studied the effect of Fe content on the diameter of CNTs produced from ferrocene-xylene mixture through chemical vapour deposition. They reported that the average Fe particle size was decreased from 35.3 to 28.2 nm with a decrease of Fe content from 0.75 to 0.075 at% and the lower Fe content resulted in the production of less CNTs. Li et al. [54] synthesised CNTs from methane and hydrogen mixture using Fe_2O_3-based catalysts with a range of 1-2nm and 3-5 nm respectively. CNTs with diameters of 1.5±0.4 nm and 3.0±0.9 nm were produced, respectively. The CNTs could be diffused by catalytic metal particles during growth process, therefore, the size of metal particles determine the diameter of filamentous carbons [53]. For example, Cheung et al. [55] used iron nanoparticles with average diameters of 3, 9, and 13nm to grow CNTs with average diameters of 3, 7, and 12 nm from ethylene, respectively.

The size of metal particles have also been reported to affect the activity of catalysts and the formation of CNTs [55-60]. In addition, loading various amounts of metal on catalyst normally results in the formation of catalyst with various metal particle sizes, as obtain in this work, to control the production of CNTs. Daudouin et al. increased the Ni loading from 1.0 wt.% to 18.5 wt.% to increase the catalytic particle sizes from 1.6 to 7.3 nm [61]. The diameter of metal particles was increased with the increase of metal loading. In addition, CNTs with larger diameters were produced with the increase of metal loading. However, a maximum diameter of CNTs should be expected, when the loading of metal in the catalyst is too high. For example, Chen et al. [62] referred to an optimally size of catalyst which could produce an optimum growth rate and a high yield

of carbon nanofibers (CNFs). They reported that smaller (< 20nm) Ni crystals caused a slow growth of CNFs and a fast deactivation of catalyst. However, when the metal particles were larger than 60nm, the rate of CNFs growth was prohibited due to the low surface area of active sites. Danafar et al.[57] studied Fe-Co/Al catalysts with 6 ranges of metal particle sizes to study the influence on the synthesis of CNTs from ethanol. They found that the catalyst with 10-20 μm metal particles produced about 30% higher carbon yield than the catalyst having the largest catalytic particles. It is reported that the catalysts with smaller diameters had larger breaking through capacities during frontal diffusion (shorter diffusion path length). In addition, the catalyst with large metal particle size produced more amorphous carbons and uninform CNTs, as the stability of metal agglomerates decreased with increasing particle sizes.

According to Table 2 and DTG-TPO (Fig. 11) analysis of the reacted catalysts with different Ni loadings, a maximum production of CNTs was obtained in the presence of the 1.0/ceramic catalyst. CNTs production was increased from 3.1 to 9.4 wt %, when the catalyst was changed from the 0.1/ceramic to the 1.0/ceramic. Similar results have been discussed by other researchers. For example, Venegoni et al. [63] studied the effect of Fe content (0.5%, 1%, 2% and 5%) on CNTs growth in the presence of Fe/SiO_2 catalysts from a mixture of H_2 and C_2H_4. Catalyst with the most amount of Fe metal content (5% $Fe\text{-}SiO_2$) was least active in relation to the production of CNTs, due to the presence of large metal particles. In addition, it was reported that the active catalytic sites was increased to promote catalytic reactions with increasing catalytic metal content until an optimal value was reached [64]. In this study, the

353 filamentous/amorphous carbon ratio was the highest about 5 with the 0.5/ceramic
354 catalyst used (Fig. 12), then slightly decreased to about 4.7 when the catalyst was
355 changed to the 1.0/ceramic. However, the 0.5/ceramic catalyst showed the highest SD
356 number (Fig. 12). Overall, considering the filamentous/amorphous carbon ratio and SD
357 of CNTs diameter, the 1.0/ceramic catalyst was suggested to be a better candidate for
358 CNTs formation from thermochemical conversion from plastic waste.

359

360 **4. Conclusions**

361 Carbon nanotubes formation from catalytic thermo-chemical conversion of waste
362 plastics using ceramic membrane based catalyst was optimized in this work in relation
363 to metal loading and reaction temperature. An optimum temperature 700^{o} was
364 suggested for Ni-based ceramics membrane. An increase of Ni content on ceramic
365 membrane resulted in increasing diameters of metal particle sizes which could affect
366 the activity of catalysts and the formation of CNTs. The 1.0/ceramic was the optimum
367 candidate for CNTs formation in this study giving the highest fraction of filamentous
368 carbons with the narrowest distribution of CNTs diameter.

369

370 **Acknowledgement**

371 The authors are grateful for the financial support from Wuhan Optics Valley
372 Environmental Technology Co., Ltd.

373

References

[1] WRAP. Plastics Market Situation Report. (Spring 2016).

[2] S.M. Al-Salem, P. Lettieri, J. Baeyens. Recycling and recovery routes of plastic solid waste (PSW): A review. Waste Management. 29 (2009) 2625-43.

[3] A. Erkiaga, G. Lopez, I. Barbarias, M. Artetxe, M. Amutio, J. Bilbao, et al. HDPE pyrolysis-steam reforming in a tandem spouted bed-fixed bed reactor for H2 production. Journal of Analytical and Applied Pyrolysis. 116 (2015) 34-41.

[4] B.B. Gershman, Inc. Gasification of Non-Recycled Plastics From Municipal Solid Waste In the United States. solid waste management consultants. GBB/12038 (2013).

[5] V.M.O.L. L.V. Radushkevich. Structure ugleroda, obrazujucegosja pri termiceskom razlozenii okisi ugleroda na zeleznom kontakte. Zurn Fisic Chim. 26 (1952) 88-95.

[6] S. Iijima. Helical microtubules of graphitic carbon. Nature. 354 (1991) 56-8.

[7] Cheaptubes. Industrial carbon nanotubes products. 2018.

[8] M. Trojanowicz. Analytical applications of carbon nanotubes: a review. TrAC Trends in Analytical Chemistry. 25 (2006) 480-9.

[9] Y. Park, T. Namioka, S. Sakamoto, T.-j. Min, S.-a. Roh, K. Yoshikawa. Optimum operating conditions for a two-stage gasification process fueled by polypropylene by means of continuous reactor over ruthenium catalyst. Fuel Processing Technology. 91 (2010) 951-7.

[10] J. Liu, Z. Jiang, H. Yu, T. Tang. Catalytic pyrolysis of polypropylene to synthesize carbon nanotubes and hydrogen through a two-stage process. Polymer Degradation and Stability. 96 (2011) 1711-9.

[11] C. Wu, L. Wang, P.T. Williams, J. Shi, J. Huang. Hydrogen production from biomass gasification with Ni/MCM-41 catalysts: Influence of Ni content. Applied Catalysis B: Environmental. 108–109 (2011) 6-13.

[12] C. Wu, P.T. Williams. Hydrogen Production from the Pyrolysis−Gasification of Polypropylene: Influence of Steam Flow Rate, Carrier Gas Flow Rate and Gasification Temperature. Energy & Fuels. 23 (2009) 5055-61.

[13] J.C. Acomb, C. Wu, P.T. Williams. The use of different metal catalysts for the simultaneous production of carbon nanotubes and hydrogen from pyrolysis of plastic feedstocks. Applied Catalysis B: Environmental. 180 (2016) 497-510.

[14] X. Liu, Y. Zhang, M.A. Nahil, P.T. Williams, C. Wu. Development of Ni- and Fe-

406 based catalysts with different metal particle sizes for the production of carbon
407 nanotubes and hydrogen from thermo-chemical conversion of waste plastics. Journal
408 of Analytical and Applied Pyrolysis.
409 [15] T.Y. Lee, J.-H. Han, S.H. Choi, J.-B. Yoo, C.-Y. Park, T. Jung, et al. Comparison
410 of source gases and catalyst metals for growth of carbon nanotube. Surface and
411 Coatings Technology. 169–170 (2003) 348-52.
412 [16] K.A. Shah, B.A. Tali. Synthesis of carbon nanotubes by catalytic chemical vapour
413 deposition: A review on carbon sources, catalysts and substrates. Materials Science in
414 Semiconductor Processing. 41 (2016) 67-82.
415 [17] Y.C. Sui, B.Z. Cui, R. Guardián, D.R. Acosta, L. Martínez, R. Perez. Growth of
416 carbon nanotubes and nanofibres in porous anodic alumina film. Carbon. 40 (2002)
417 1011-6.
418 [18] S.D. Mhlanga, K.C. Mondal, R. Carter, M.J. Witcomb, N.J. Coville. The effect of
419 synthesis parameters on the catalytic synthesis of multiwalled carbon nanotubes using
420 Fe-Co/CaCO3 catalysts. South African Journal of Chemistry. 62 (2009) 67-76.
421 [19] M. Kumar, Y. Ando. Controlling the diameter distribution of carbon nanotubes
422 grown from camphor on a zeolite support. Carbon. 43 (2005) 533-40.
423 [20] H. Ago, N. Uehara, N. Yoshihara, M. Tsuji, M. Yumura, N. Tomonaga, et al. Gas
424 analysis of the CVD process for high yield growth of carbon nanotubes over metal-
425 supported catalysts. Carbon. 44 (2006) 2912-8.
426 [21] G. Bajad, V. Guguloth, R.P. Vijayakumar, S. Bose. Conversion of plastic waste
427 into CNTs using Ni/Mo/MgO catalystAn optimization approach by mixture experiment.
428 Fullerenes Nanotubes and Carbon Nanostructures. 24 (2016) 162-9.
429 [22] N. Borsodi, A. Szentes, N. Miskolczi, C. Wu, X. Liu. Carbon nanotubes
430 synthetized from gaseous products of waste polymer pyrolysis and their application.
431 Journal of Analytical and Applied Pyrolysis. 120 (2016) 304-13.
432 [23] G. Che, B.B. Lakshmi, C.R. Martin, E.R. Fisher, R.S. Ruoff. Chemical Vapor
433 Deposition Based Synthesis of Carbon Nanotubes and Nanofibers Using a Template
434 Method. Chemistry of Materials. 10 (1998) 260-7.
435 [24] H.M. Cheng, F. Li, G. Su, H.Y. Pan, L.L. He, X. Sun, et al. Large-scale and low-
436 cost synthesis of single-walled carbon nanotubes by the catalytic pyrolysis of
437 hydrocarbons. Applied Physics Letters. 72 (1998) 3282-4.
438 [25] M. Golshadi, J. Maita, D. Lanza, M. Zeiger, V. Presser, M.G. Schrlau. Effects of

synthesis parameters on carbon nanotubes manufactured by template-based chemical vapor deposition. Carbon. 80 (2014) 28-39.
[26] Z.F. Ren, Z.P. Huang, J.W. Xu, J.H. Wang, P. Bush, M.P. Siegal, et al. Synthesis of large arrays of well-aligned carbon nanotubes on glass. Science (New York, NY). 282 (1998) 1105-7.
[27] W. Zhao, B. Basnet, I.J. Kim. Carbon nanotube formation using zeolite template and applications. Journal of Advanced Ceramics. 1 (2012) 179-93.
[28] X. Liu, H. Sun, C. Wu, D. Patel, J. Huang. Thermal Chemical Conversion of High-Density Polyethylene for the Production of Valuable Carbon Nanotubes Using Ni/AAO Membrane Catalyst2017.
[29] M. Lee, B. Wang, Z. Wu, K. Li. Formation of micro-channels in ceramic membranes – Spatial structure, simulation, and potential use in water treatment. Journal of Membrane Science. 483 (2015) 1-14.
[30] E.T. Thostenson, Z. Ren, T.-W. Chou. Advances in the science and technology of carbon nanotubes and their composites: a review. Composites Science and Technology. 61 (2001) 1899-912.
[31] N. Labhsetwar, P. Doggali, S. Rayalu, R. Yadav, T. Mistuhashi, H. Haneda. Ceramics in Environmental Catalysis: Applications and Possibilities. Chinese Journal of Catalysis. 33 (2012) 1611-21.
[32] C. Quan, N. Gao, C. Wu. Utilization of NiO/porous ceramic monolithic catalyst for upgrading biomass fuel gas. Journal of the Energy Institute.
[33] N. Gao, S. Liu, Y. Han, C. Xing, A. Li. Steam reforming of biomass tar for hydrogen production over NiO/ceramic foam catalyst. International Journal of Hydrogen Energy. 40 (2015) 7983-90.
[34] Y. Liu, M. Peng, H. Jiang, W. Xing, Y. Wang, R. Chen. Fabrication of ceramic membrane supported palladium catalyst and its catalytic performance in liquid-phase hydrogenation reaction. Chemical Engineering Journal. 313 (2017) 1556-66.
[35] J.W. An, D.H. You, D.S. Lim. Tribological properties of hot-pressed alumina–CNT composites. Wear. 255 (2003) 677-81.
[36] E. Flahaut, A. Peigney, C. Laurent, C. Marlière, F. Chastel, A. Rousset. Carbon nanotube–metal–oxide nanocomposites: microstructure, electrical conductivity and mechanical properties. Acta Materialia. 48 (2000) 3803-12.
[37] V. Muñoz, A.G.T. Martinez. Thermal Evolution of Al2O3-MgO-C Refractories.

Procedia Materials Science. 1 (2012) 410-7.
[38] J. Zygmuntowicz, P. Wiecińska, A. Miazga, K. Konopka. Characterization of composites containing NiAl2O4 spinel phase from Al2O3/NiO and Al2O3/Ni systems. Journal of Thermal Analysis and Calorimetry. 125 (2016) 1079-86.
[39] C. Wu, M.A. Nahil, M. Norbert, J. Huang, P.T. Williams. Production and application of carbon nanotubes, as a co-product of hydrogen from the pyrolysis-catalytic reforming of waste plastic. Process Safety and Environmental Protection.
[40] W.Z. Li, J.G. Wen, Z.F. Ren. Effect of temperature on growth and structure of carbon nanotubes by chemical vapor deposition. Applied Physics A. 74 (2002) 397-402.
[41] G.L. Hornyak, A.C. Dillon, P.A. Parilla, J.J. Schneider, N. Czap, K.M. Jones, et al. Template synthesis of carbon nanotubes. Nanostructured Materials. 12 (1999) 83-8.
[42] A. Aqel, K.M.M.A. El-Nour, R.A.A. Ammar, A. Al-Warthan. Carbon nanotubes, science and technology part (I) structure, synthesis and characterisation. Arabian Journal of Chemistry. 5 (2012) 1-23.
[43] F. Danafar, A. Fakhru'l-Razi, M.A.M. Salleh, D.R.A. Biak. Fluidized bed catalytic chemical vapor deposition synthesis of carbon nanotubes—A review. Chemical Engineering Journal. 155 (2009) 37-48.
[44] B.R. Stoner, B. Brown, J.T. Glass. Selected Topics on the Synthesis, Properties and Applications of Multiwalled Carbon Nanotubes. Diamond and related materials. 42 (2014) 49-57.
[45] K.-E. Kim, K.-J. Kim, W.S. Jung, S.Y. Bae, J. Park, J. Choi, et al. Investigation on the temperature-dependent growth rate of carbon nanotubes using chemical vapor deposition of ferrocene and acetylene. Chemical Physics Letters. 401 (2005) 459-64.
[46] C.J. Lee, J. Park, Y. Huh, J. Yong Lee. Temperature effect on the growth of carbon nanotubes using thermal chemical vapor deposition. Chemical Physics Letters. 343 (2001) 33-8.
[47] N. Mishra, G. Das, A. Ansaldo, A. Genovese, M. Malerba, M. Povia, et al. Pyrolysis of waste polypropylene for the synthesis of carbon nanotubes. Journal of Analytical and Applied Pyrolysis. 94 (2012) 91-8.
[48] C. Wu, P.T. Williams. Pyrolysis–gasification of post-consumer municipal solid plastic waste for hydrogen production. International Journal of Hydrogen Energy. 35 (2010) 949-57.
[49] J.C. Acomb, C. Wu, P.T. Williams. Effect of growth temperature and

feedstock:catalyst ratio on the production of carbon nanotubes and hydrogen from the pyrolysis of waste plastics. Journal of Analytical and Applied Pyrolysis. 113 (2015) 231-8.

[50] A.F.l.-R. Hengameh Hanaei1, 2,*, Dayang Radiah Awang Biak2, Intan Salwani Ahamad2 and Firoozeh Danafar. Effects of Synthesis Reaction Temperature, Deposition Time and Catalyst on Yield of Carbon Nanotubes. Asian Journal of Chemistry. 24 (2010) 2407-14.

[51] T. Setareh Monshi, A. Fakhru'l-Razi, A. Luqman Chuah, A.R. Suraya. Optimization of Synthesis Condition for Carbon Nanotubes by Catalytic Chemical Vapor Deposition (CCVD). IOP Conference Series: Materials Science and Engineering. 17 (2011) 012003.

[52] E.F. Kukovitsky, S.G. L'Vov, N.A. Sainov, V.A. Shustov, L.A. Chernozatonskii. Correlation between metal catalyst particle size and carbon nanotube growth. Chemical Physics Letters. 355 (2002) 497-503.

[53] S.B. Sinnott, R. Andrews, D. Qian, A.M. Rao, Z. Mao, E.C. Dickey, et al. Model of carbon nanotube growth through chemical vapor deposition. Chemical Physics Letters. 315 (1999) 25-30.

[54] Y. Li, W. Kim, Y. Zhang, M. Rolandi, D. Wang, H. Dai. Growth of Single-Walled Carbon Nanotubes from Discrete Catalytic Nanoparticles of Various Sizes. The Journal of Physical Chemistry B. 105 (2001) 11424-31.

[55] C.L. Cheung, A. Kurtz, H. Park, C.M. Lieber. Diameter-Controlled Synthesis of Carbon Nanotubes. The Journal of Physical Chemistry B. 106 (2002) 2429-33.

[56] A.L.M. da Silva, J.P. den Breejen, L.V. Mattos, J.H. Bitter, K.P. de Jong, F.B. Noronha. Cobalt particle size effects on catalytic performance for ethanol steam reforming – Smaller is better. Journal of Catalysis. 318 (2014) 67-74.

[57] F. Danafar, A. Fakhru'l-Razi, M.A. Mohd Salleh, D.R. Awang Biak. Influence of catalytic particle size on the performance of fluidized-bed chemical vapor deposition synthesis of carbon nanotubes. Chemical Engineering Research and Design. 89 (2011) 214-23.

[58] A. Gorbunov, O. Jost, W. Pompe, A. Graff. Role of the catalyst particle size in the synthesis of single-wall carbon nanotubes. Applied Surface Science. 197–198 (2002) 563-7.

[59] C. Lastoskie, K.E. Gubbins, N. Quirke. Pore size distribution analysis of

538 microporous carbons: a density functional theory approach. The Journal of Physical
539 Chemistry. 97 (1993) 4786-96.
540 [60] R.J.W. R.T.K. Baker. Formation of carbonaceous deposits from the platinum-iron
541 catalyzed decomposition of acetylene. Journal of Catalysis. 37 (1975) 101-5.
542 [61] D. Baudouin, U. Rodemerck, F. Krumeich, A.d. Mallmann, K.C. Szeto, H. Ménard,
543 et al. Particle size effect in the low temperature reforming of methane by carbon dioxide
544 on silica-supported Ni nanoparticles. Journal of Catalysis. 297 (2013) 27-34.
545 [62] D. Chen, K.O. Christensen, E. Ochoa-Fernández, Z. Yu, B. Tøtdal, N. Latorre, et
546 al. Synthesis of carbon nanofibers: effects of Ni crystal size during methane
547 decomposition. Journal of Catalysis. 229 (2005) 82-96.
548 [63] D. Venegoni, P. Serp, R. Feurer, Y. Kihn, C. Vahlas, P. Kalck. Parametric study for
549 the growth of carbon nanotubes by catalytic chemical vapor deposition in a fluidized
550 bed reactor. Carbon. 40 (2002) 1799-807.
551 [64] F. Melo, N. Morlanés. Naphtha steam reforming for hydrogen production.
552 Catalysis Today. 107–108 (2005) 458-66.

553

554

555

556

Table 1 - ICP results of Ni/ceramic catalysts with different Ni contents				
catalysts	0.1 / ceramic	0.5 / ceramic	1.0 / ceramic	2.0 / ceramic
Ni content wt.%	0.25	1.1	2.1	3.3

583

584

Table 2 – Overall view of experiments parameters and carbon depositions

	Ni Content ($molL^{-1}$)	Temperature ($°C$)	Amorphous Carbon ($\%$)	Filamentous Carbon ($\%$)	CNTs Average Diameter (nm)
Effect of the Ni content	0.1	700	1.1	3.1	15.7 ± 3.6
	0.5	700	1.2	6.0	16.9 ± 4.3
	1.0	700	2.0	9.4	20.8 ±1.9
	2.0	700	2.2	8.0	24.9 ± 2.3
Effect of temperature	0.5	600	2.1	7.2	21.2 ± 5.6
	0.5	700	1.2	6.0	16.9 ± 4.3
	0.5	800	1.2	1.2	-

585

586

587

588

589

590

591

592

593

594

595

596

597

598

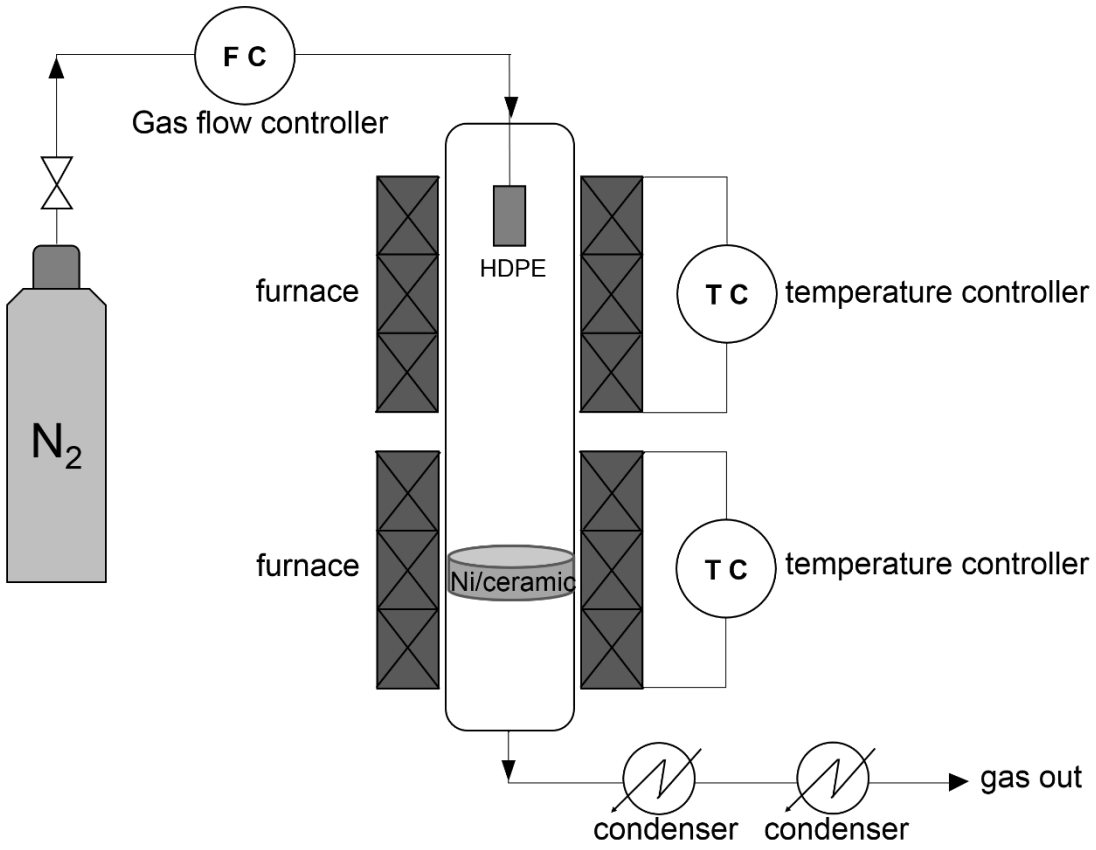

599

600 Fig. 1 A schematic diagram of the reactor for the synthesis CNTs from waste plastics

601

602

603

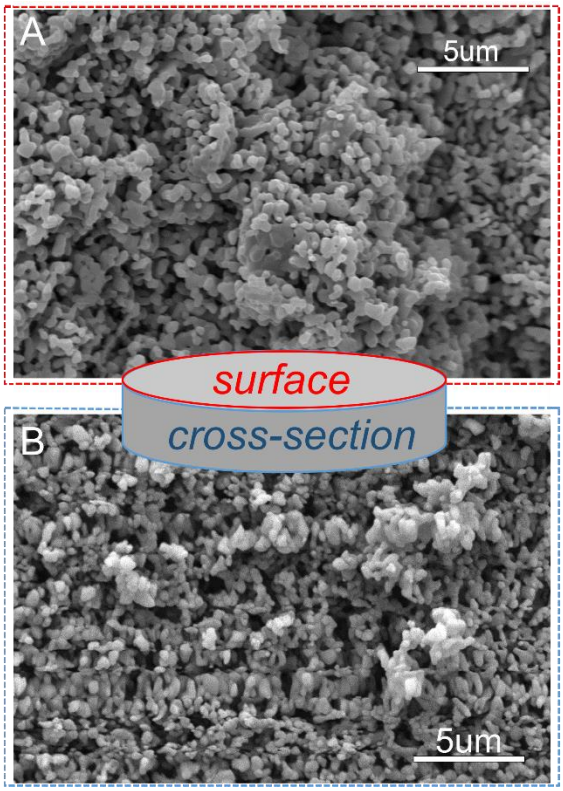

Fig. 2 SEM results for original ceramic membrane (A) surface, (B) cross-section

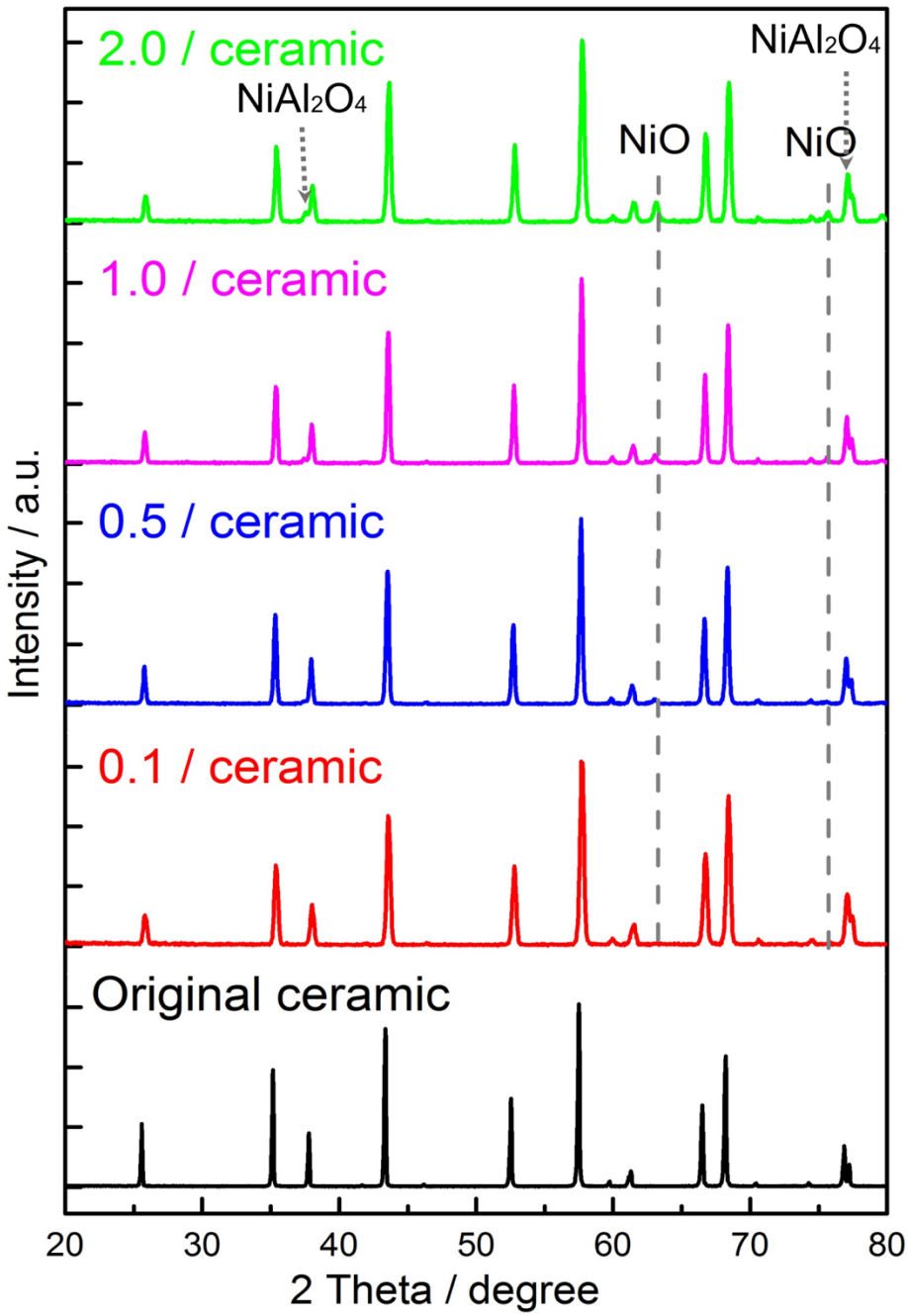

607

608 Fig. 3 XRD analysis for original ceramic membrane and fresh Ni/ceramic catalysts

609

610

611

612

613

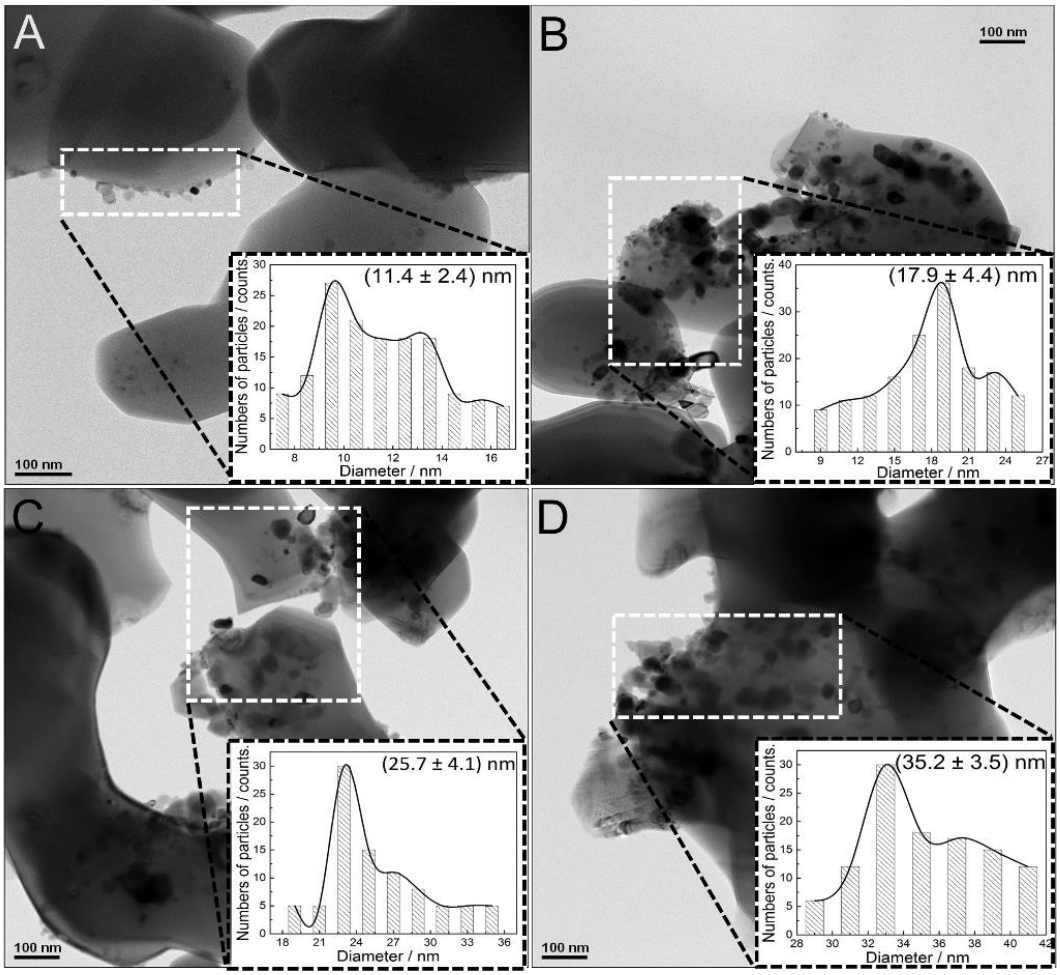

614

615 Fig. 4 TEM results and diameter distribution of NiO for (A) 0.1, (B) 0.5, (C) 1.0 and

616 (D) 2.0 fresh Ni/ceramic catalysts

617

618

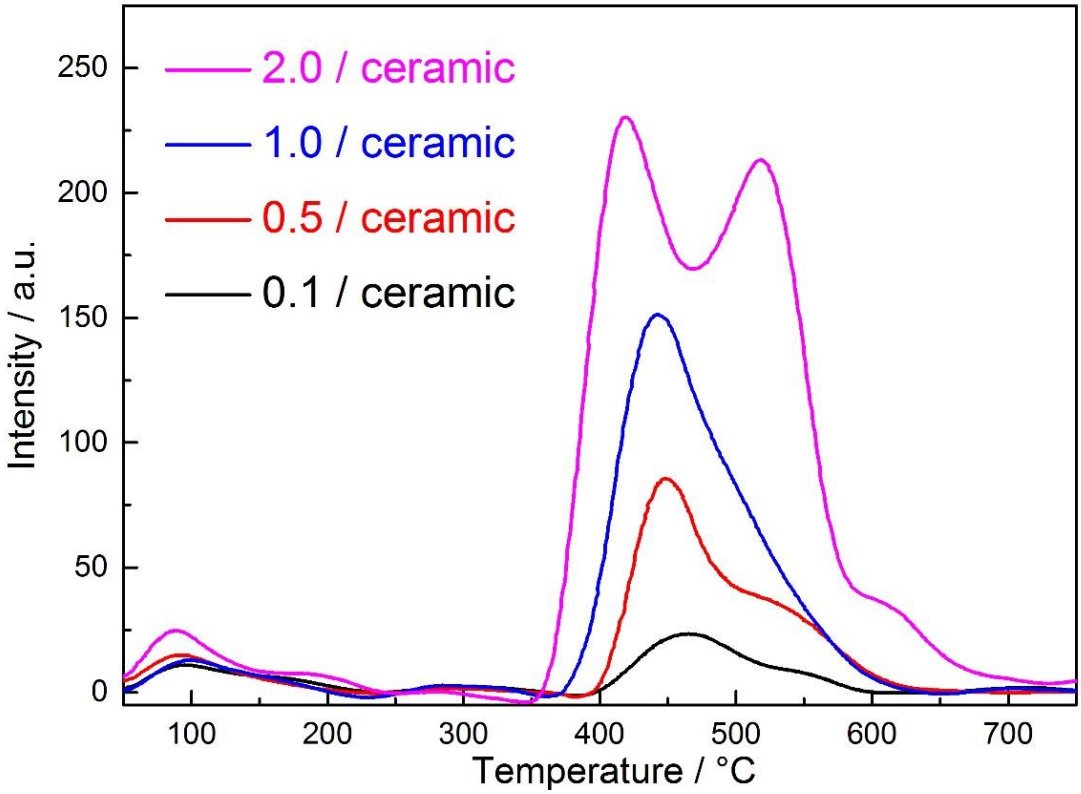

Fig. 5 TPR analysis of the Ni/ceramic catalysts with different Ni content loadings (0.1, 0.5, 1.0, and 2.0 Ni mol/L)

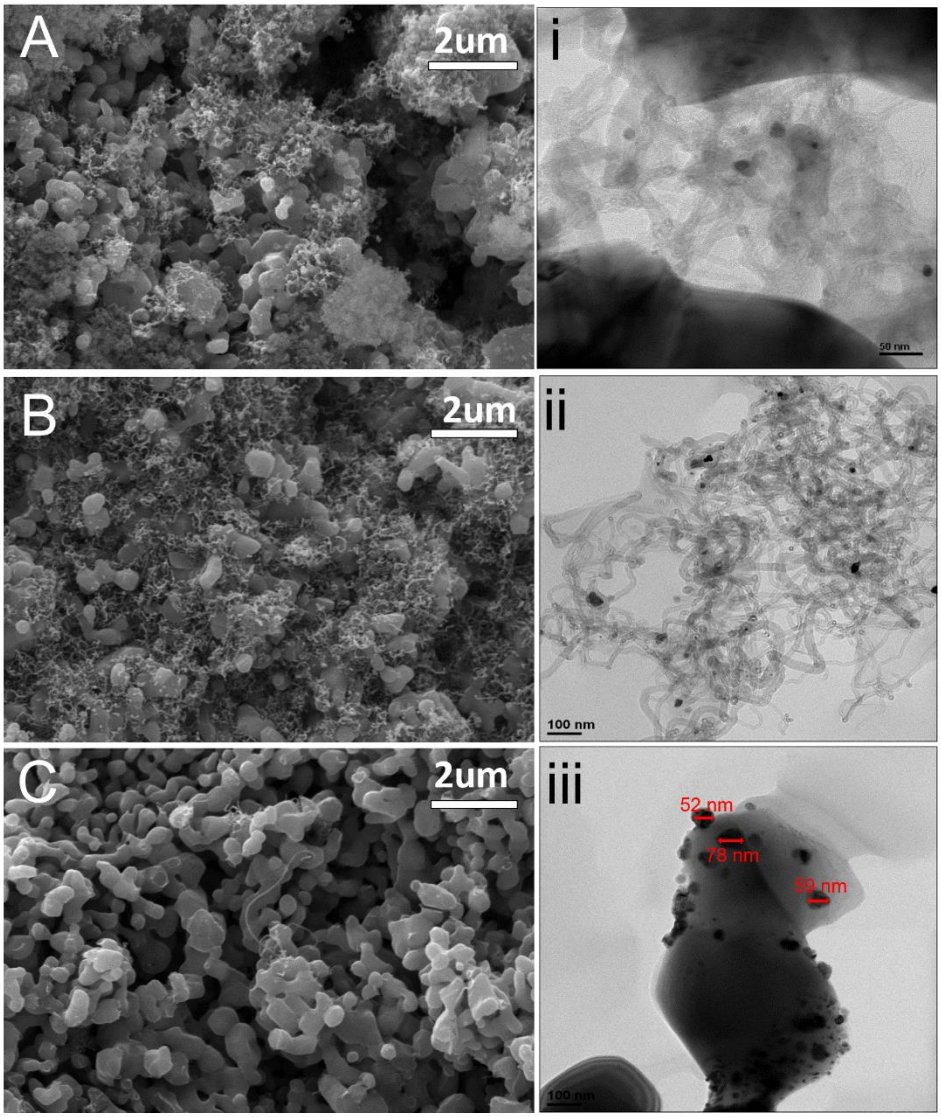

630

631 Fig. 6 SEM (left) and TEM (right) results for CNTs synthesis at (A) 600°C, (B) 700°C

632 and (C) 800°C

633

634

635

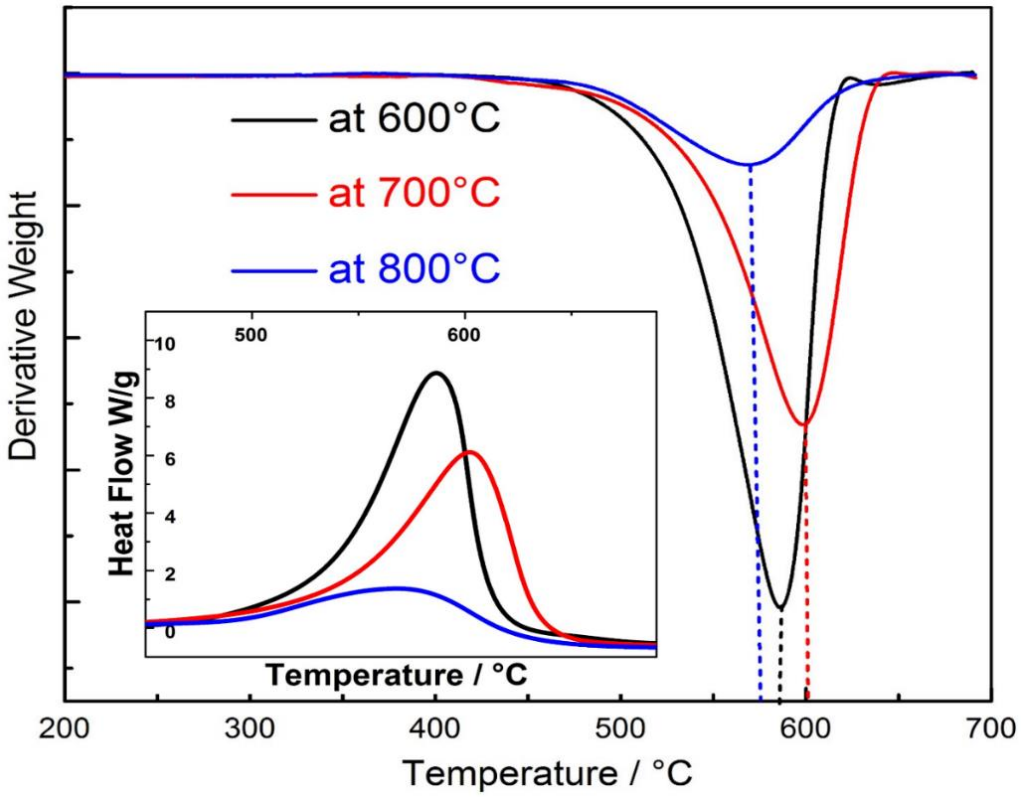

636

637 Fig. 7 DTG-TPO and DSC results of the spent 0.5/ceramic at 600 °C, 700 °C, and

638 800 °C

639

640

641

642

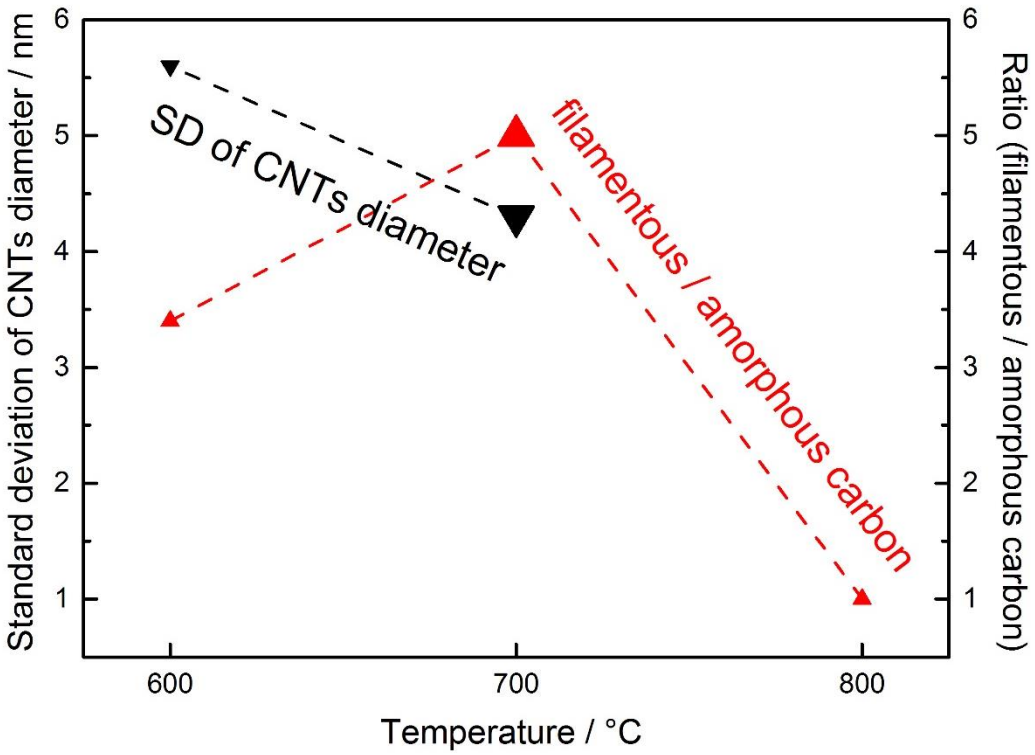

643

644 Fig. 8 Trends of standard deviation (SD) of CNTs diameter and

645 filamentous/amorphous carbon ratio at 600 °C, 700 °C, and 800 °C

646

647

648

649

650

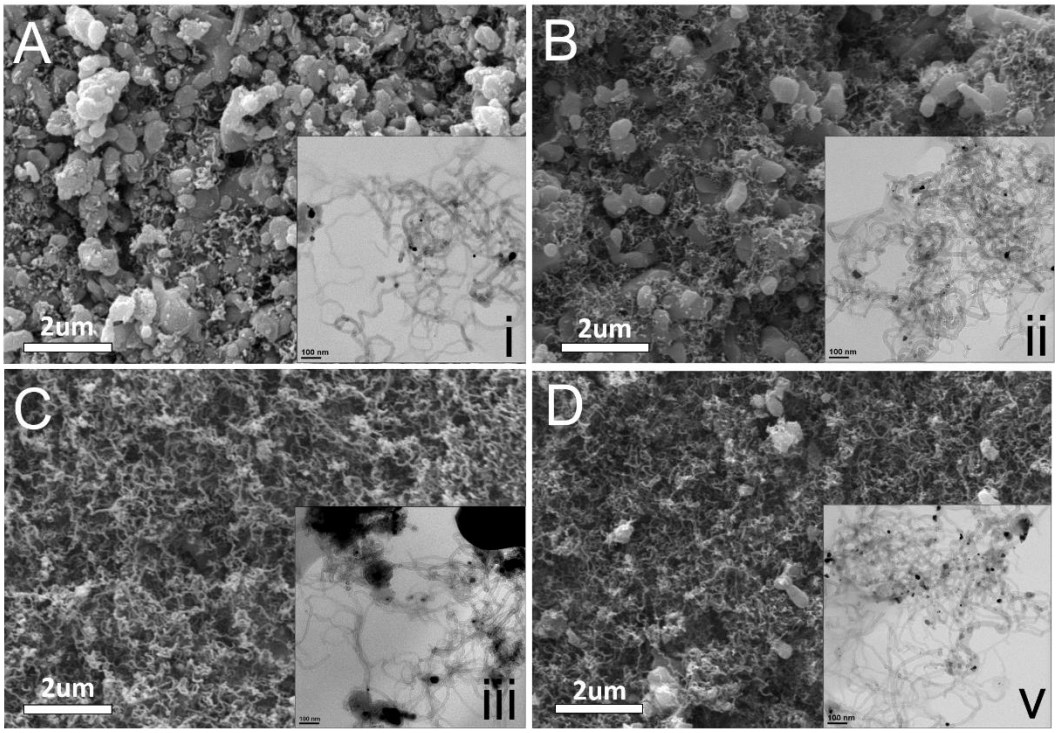

651

652 Fig. 9 SEM results of CNTs formation for 0.1/ceramic (A), 0.5/ceramic (B),

653 1.0/ceramic (C), and 2.0/ceramic (D) and corresponding TEM (i-v)

654

655

656

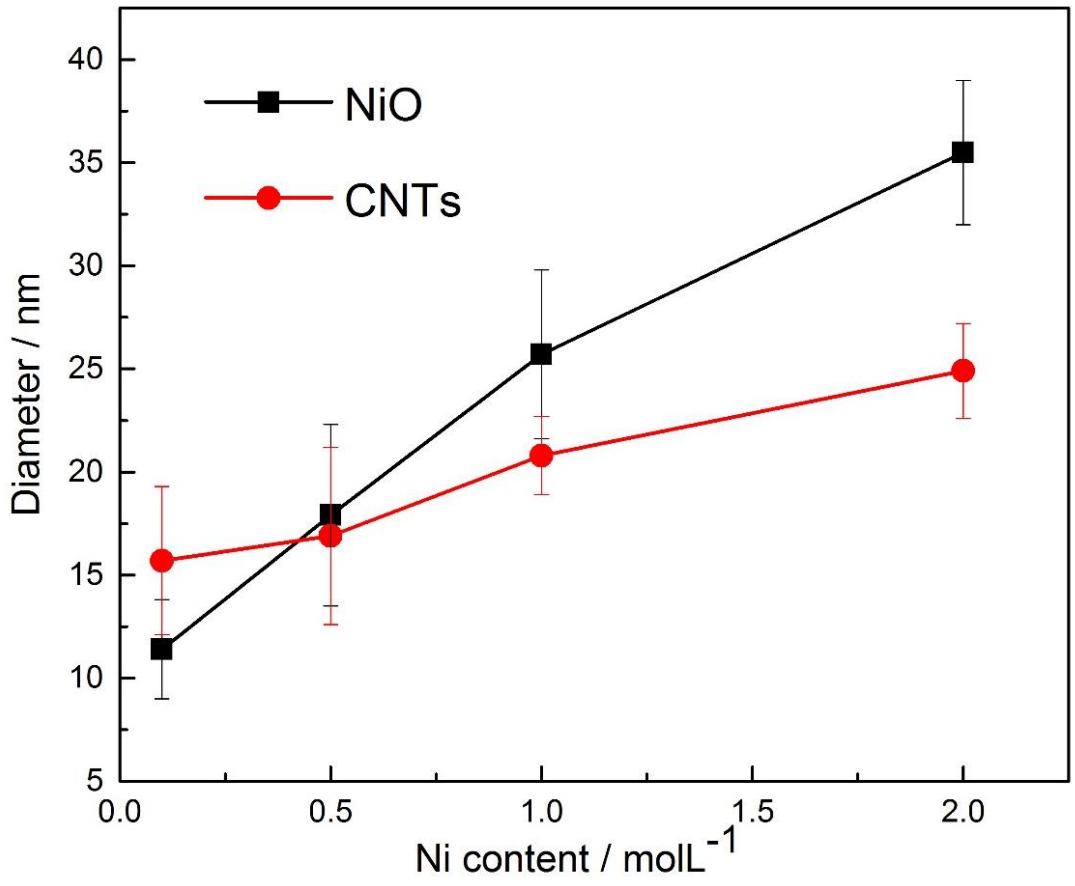

657

658 Fig. 10 Diameter distribution comparison for fresh and spent Ni/ceramic catalysts

659

660

661

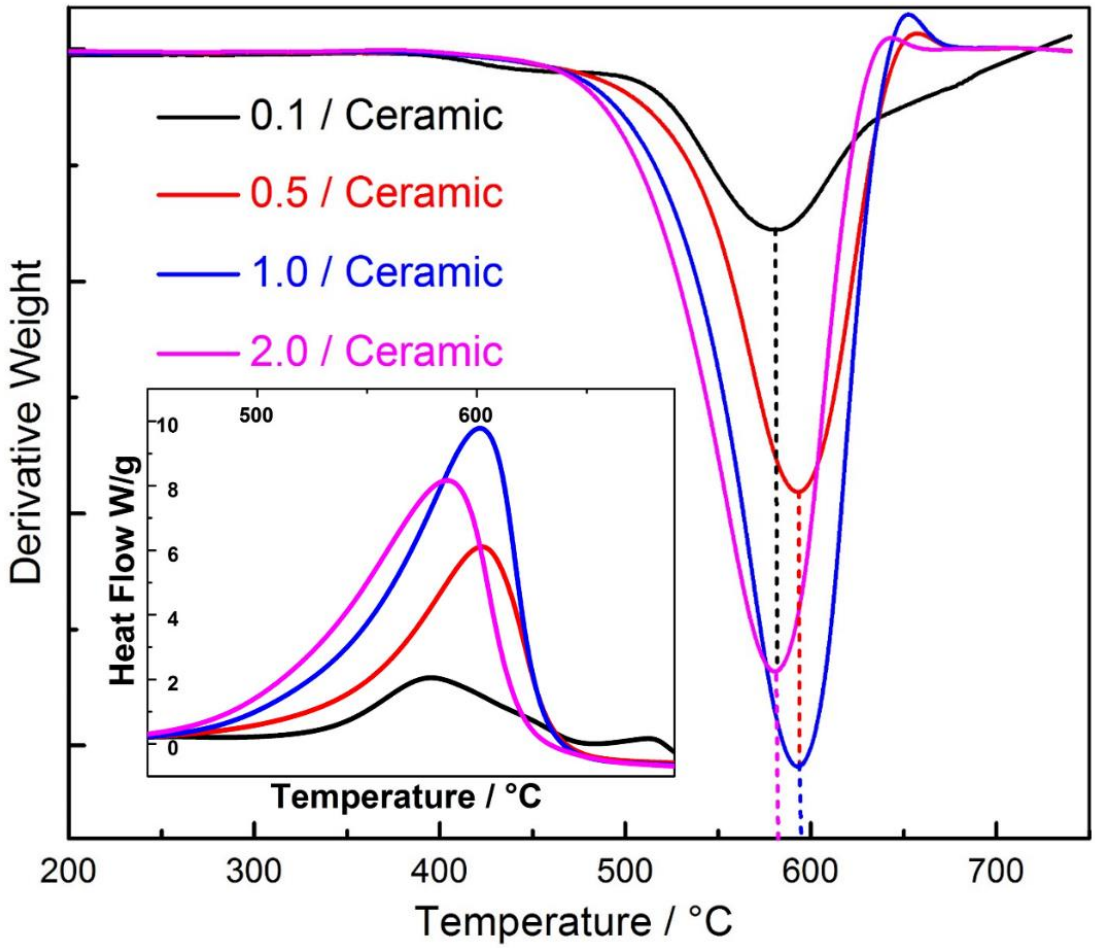

662

663 Fig. 11 DTG-TPO and DSC results of the spent 0.1/ceramic, 0.5/ceramic, 1.0/ceramic

664 and 2.0/ceramic catalysts at 700 °C

665

666

667

668

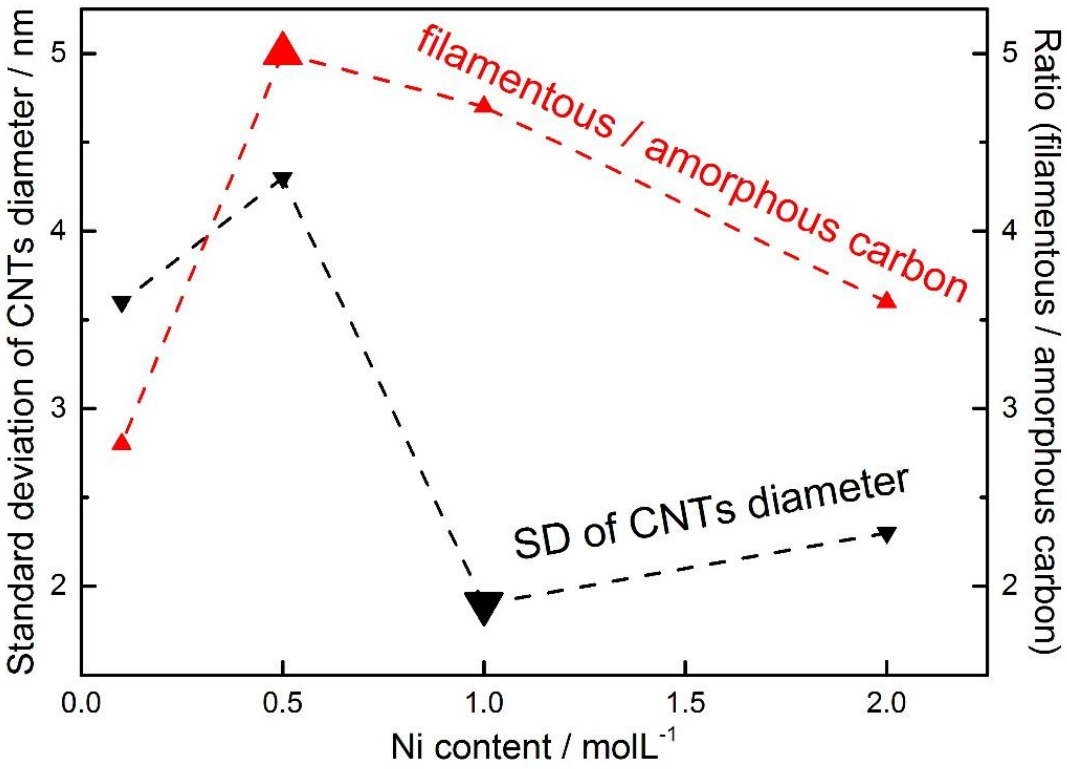

669

670 Fig. 12 Trends of standard deviation (SD) of CNTs diameter and

671 filamentous/amorphous carbon ratio with different Ni loading ceramic catalysts

672